International Science and Technology Journal
المجلة الدولية للعلوم والتقنية
Volume 36 العدد
Part 1 المجلد
http://www.doi.org/10.62341/sksp2112

Received	2025/01/28	تم استلام الورقة العلمية في
Accepted	2025/02/25	تم قبول الورقة العلمية في
Published	2025/02/27	تم نشر الورقة العلمية في

Physical and Mathematical Modeling of Bending and Twisting Due to Vibration on Flat Wings

[1]Kamel Y. Youssef , [2]Salahaddin M. Sahboun, [3]Shaker M. Shaabo

[1]Lecturer, Department of Aeronautical Mechanics Engineering, Faculty of Aeronautical Sciences, Bright Star University, City: El-Brega - Libya .E-mail: engkamelyoussef@gmail.com

[2]Director of Entrepreneurship & Innovation Center Bright Star University, City: El-Brega - Libya.

E-mail: s.sahboun@bsu.edu.ly

[3]Lecturer Department of physics, Faculty of Petroleum Engineering, Aljufra University, Zella, Libya.

Email: shaboshaker@gmail.com

Abstract.

In this research, the phenomenon of flutter and bending in aircraft wings was studied. In the first part, this phenomenon was defined in general, the causes leading to it, and the problems resulting from it, along with an introduction to the importance of studying it and finding appropriate solutions for it, in addition to some reference studies about it. In the second part, the explanation of the phenomenon of aeroelasticity was expanded upon, and a historical overview of its appearance and the experiments conducted on it was provided, in addition to the definition of static aeroelasticity, such as the static aeroelastic behavior of a Fixed Root Flexible Wing {the lift coefficient for 3D wing and the effect of AR on Cl versus angle of attack graph. The typical effect of a (negative) twist angle on the lift distribution. As well as the Twist Angle and its effect on the lift distribution, in addition to Twist and Divergence of the Fixed Root Flexible Wing. Dynamic Aeroelasticity is also explained: Flutter instability, Types of Flutter and the effect of spacing and wind speed on the Flutter. The third part dealt with methods of flutter control for wings and Panels, explaining some of these methods and the experiments conducted by researchers in this field. A computer

http://www.doi.org/10.62341/sksp2112

simulation conducted on one of the engineering programs {MATLAB, and ANSYS} of one of the damping methods to stabilize the aircraft, avoid flutter at different speeds, and determine the best speed according to the Mach number.

Key Words: flutter, aeroelasticity, Twist, Divergence, Flutter instability, computer simulation, engineering programs, damping, aircraft.

النمذجة الفيزيائية والرياضية للانحناء والالتواء بسبب الاهتزاز على الاجنحة المسطحة

[1]كامل يحي يوسف، [2]صلاح الدين مصباح سحبون، [3]شعبوا محمود شاكير

[1]كلية علوم الطيران، جامعة النجم الساطع، [2]مركز الريادة والابتكار، جامعة النجم الساطع، [3]كلية البترول، جامعة الجفرة

الملخص

تم في هذا البحث دراسة ظاهرة الرفرفة والانحناء في اجنحة الطائرات. في الجزء الاول تعريف لهذة الظاهرة بشكل عام، والاسباب المؤدية اليها، والمشاكل الناتجة عنها، مع مقدمة لأهمية دراستها وايجاد الحلول المناسبة لها. بالإضافة الى بعض الدراسات المرجعية حولها. في الجزء الثاني تم التوسع في شرح ظاهرة المرونة الهوائية، وتقديم نبذة عن ظهورها والتجارب التي اجريت عليها، بالإضافة الى تعريف المرونة الساكنة، مثل سلوك المرونة الهوائية الساكنة لجسم ثابت. الجناح المرن الجذري (معامل الرفع للجناح ثلاثي الابعاد مقابل زاوية CL على الرسم البياني AR و تأثير الهجوم الهوائي). التأثير النموذجي لزاوية الالتواء وتأثيرها على توزيع الرفع، بالإضافة الى الالتواء والتباعد للجناح المرن ذو الجذر الثابت. كما تم شرح المرونة الهوائية الديناميكية: عدم استقرار الرفرفة، انواع الرفرفة وتأثير التباعد وسرعة الرياح على الرفرفة، اما الجزء الثالث فقد تناول طرق التحكم في الجنحة والألواح، موضحا بعض هذه الطرق والتجارب التي اجراها الباحثون في هذا المجال. محاكاة حاسوبية اجريت على أحد البرامج الهندسية MATLAB لاحد طرق التحليل لتثبيت الطائرة ANSYS وتجنب الرفرفة عند السرعات المختلفة وتحديد السرعة الافضل.

http://www.doi.org/10.62341/sksp2112

الكلمات المفتاحية: الرفرفة، المرونة الهوائية، الالتواء، التباعد، المرونة الهوائية الديناميكية، المحاكاة الحاسوبية، الطائرة.

1. Introduction.

Aviation is considered one of the most widely used means of transportation in the world, and it is one of the methods that require comprehensive study to achieve the required safety. One of the most important parts of the aircraft is its wings, which help in flying and keeping the aircraft in the air for a long period. One of the problems that can affect the aircraft's wings is flutter and distortion. Flutter is arguably the most important of all the aeroelastic phenomena and is the most difficult to predict. It is an unstable self-excited vibration in which the structure extracts energy from the air stream and often results in catastrophic structural failure [1,2].

As for the bending in the wings of the aircraft, it is the bending of the aircraft's wings because of the forces acting on them, and external factors such as the loads resulting from winds, landing, and takeoff, in addition to the horizontal pressure forces affecting the aircraft parts [3, 4, 5].

2. Causes of Flutter and Wing Deformation in Aircraft.

Several factors affect the occurrence of flutter and wing deformation in aircraft, ranging from the aerodynamic to the mechanical characteristics of the aircraft. Here are some key factors [5, 6, 7].

Aircraft speed: As the speed of the aircraft increases, the chances of flutter and wing deformation increase due to the increased pressure on the wings.

1. Aircraft design: The design of the aircraft may lead to exceeding the limits of flutter and wing deformation, resulting in aircraft failure.
2. Aircraft weight: As the weight of the aircraft increases, the chances of flutter and wing deformation increase due to the increased load on the wings.
3. Weather conditions: Winds, turbulence, and turbulent air can lead to flutter and wing deformation.

3. Reference Studies:

The aeroelastic stability of air-craft wings has been an active project topic since the beginning of the 19th century, one of the first studies that dealt with flutter analysis was pre-sented by Bairstow and Fage [8] describing the investigation into the flutter instability that occurred in the horizontal tail of the twin-engined Handley Page

http://www.doi.org/10.62341/sksp2112

O/400. Goland [9] studied the flutter of a uniform aircraft wing through integration of the governing differential equations. Goland and Luke studied the effect of adding wing-tip weights on the flutter of the wing[10]. The shape of the wing planform is one of the important factors that derives the performance characteristics of aircraft. Usually, the planform shape of the wing is a trade-off between different flight conditions and is not always the optimized shape for each flight condition. Therefore, the idea of changing the wing planform in flight to op-timize the shape of the wing in each flight condition has been proposed [11, 12]. Morphing wings enhance the performance of the wing by changing the shape of lifting surfaces using some form of mechanism [11, 12]; however, any change in the wing planform might affect the aeroelastic behaveour of the wing. Therefore, the aeroe-lastic stability of such wings should also be considered in a flight configuration.

4. Dynamic Aeroelasticity.

Dynamic aeroelasticity concerns the interaction between inertia as it shown in fig 1, elastic, and unsteady aerodynamic forces. This dynamic problem is more complex than static aeroelasticity, since vibration of the structure is also involved. Flutter is an important dynamic aeroelasticity phenomenon [5, 6].

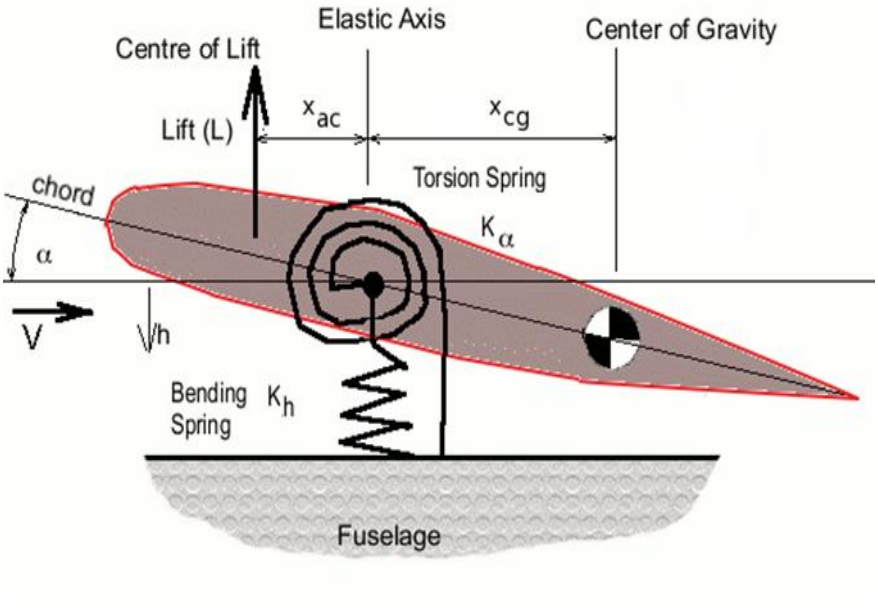

Fig 1: Dynamic aeroelasticity

http://www.doi.org/10.62341/sksp2112

5. Mathematical Model

5.1. models of elastic-flexural wing flutter.

Equations of bending and twisting of a flat wing. The physical system under consideration is a two-dimensional section of a wing undergoing pitch and plunge oscillations (plunge), Fig 2. The inclination angle relative to the elastic axis is denoted by the letter α (positive when the leading edge is facing upwards). The bend, denoted by, is positive in the downward direction. The elastic axis is located at a distance a_hb from the middle chord of the wing, and the center of mass is located at a distance x_αb from the elastic axis. Both distances are positive when measured to the trailing edge of the wing profile.

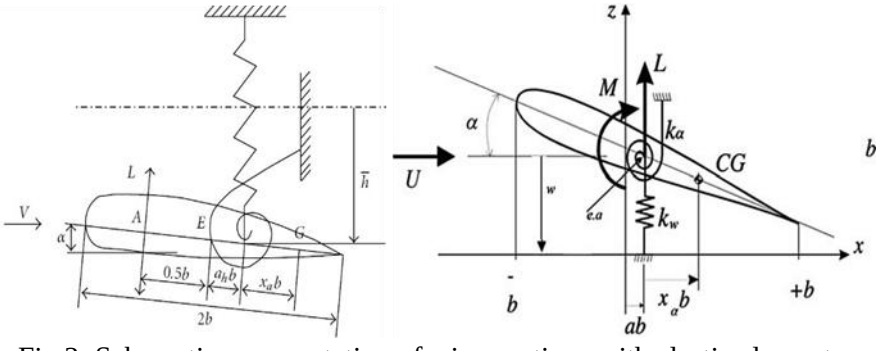

Fig 2: Schematic representation of wing sections with elastic elements

For cubic restoring forces with subsonic aerodynamics, the related equations for wing deflection.

$$\begin{bmatrix} I_\alpha & m_w x_\alpha b \\ m_w x_\alpha b & m_t \end{bmatrix} \begin{bmatrix} \ddot{\alpha} \\ \ddot{h} \end{bmatrix} + \begin{bmatrix} c_\alpha & 0 \\ 0 & c_h \end{bmatrix} \begin{bmatrix} \dot{\alpha} \\ \dot{h} \end{bmatrix} + \begin{bmatrix} k_\alpha(\alpha) & 0 \\ 0 & k_h(h) \end{bmatrix} \begin{bmatrix} \alpha \\ h \end{bmatrix} = \begin{bmatrix} M \\ -L \end{bmatrix} \quad (1)$$

Where:

m_t: total mass of the main wing and supporting structure

m_w: mass of the main wing

x_α: dimensionless distance between the center of mass and the axis of bending;

I_α: moment of inertia of the structure

b: mean aerodynamic chord (MAC) of the wing [13, 14, 15]

c_α, c_h: damping coefficients for bending displacement and pitch angle respectively

http://www.doi.org/10.62341/sksp2112

$k_h(h)$ and $k_\alpha(\alpha)$: displacement and angular stiffness coefficients of the wing respectively
$\alpha k_\alpha(\alpha)$: nonlinear term of the elasticity force, which is determined by the expression [16].

$$\alpha k_\alpha(\alpha) = k_1\alpha^2 + k_2\alpha^3 \quad (2)$$

In, the elasticity coefficient is taken in the form of $k_\alpha(\alpha)=k_{\alpha 0}+k_{\alpha 1}\alpha+k_{\alpha 2}\alpha^2$. According to, the aerodynamic terms L, M (lift and torque respectively) at low frequencies and in subsonic flight can be expressed using the Theodorsen approximation [13, 14] in the form

$$L = \&\rho V^2 b c_{l_\alpha} s_p \left(\alpha + \left(\frac{\dot{h}}{V} + \left(\frac{1}{2} - A\right) b \frac{\alpha}{V}\right)\right) + \rho V^2 b c_{l_\beta} s_p + \rho V^2 b c_{l_\gamma} s_p \gamma \quad (3)$$

$$M = \&\rho V^2 b^2 c_{m_{\alpha-\text{eff}}} s_{p|} \left(\alpha + \left(\frac{\dot{h}}{V} + \left(\frac{1}{2} - A\right) b \frac{\alpha}{V}\right)\right) + \rho V^2 b^2 c_{m_{\beta-\text{eff}}} s_p \beta + \rho V^2 b^2 c_{m_{\gamma-\text{eff}}} s_p \gamma \quad (4)$$

Where:
ρ: air density
V: flight airspeed
a: relative distance between the elastic axis and the MAC of the wing (this parameter significantly affects the stability of the system)
s_p: wing span
$c_{l\alpha}$, $c_{m\alpha}$: lift and moment coefficients per unit angle of attack (lift and moment derivatives with respect to angle of attack)
$c_{l\beta}$, $c_{m\beta}$: lift and moment coefficients per unit angle of attack along the trailing edge of the wing
$c_{l\gamma}$, $c_{m\gamma}$: lift and moment coefficients per unit angle of attack along the leading edge of the wing
$c_{m\alpha\text{-eff}}$, $c_{m\beta\text{-eff}}$, $c_{m\gamma\text{-eff}}$: denote derivatives of the aerodynamic moment with respect to angles of attack: wing, trailing edge, and leading edge of the wing respectively. According to [16], the parameters of this model are defined by the following expressions:

http://www.doi.org/10.62341/sksp2112

$$
\begin{aligned}
c_{m_{\alpha-\text{ eff}}} &= \left(\frac{1}{2}+a\right)c_{l_\alpha}+2c_{m_\alpha}\\
c_{m_{\beta-\text{eff}}} &= \left(\frac{1}{2}+a\right)c_{\beta}+2c_{m_\beta}\\
c_{m_{\gamma-\text{eff}}} &= \left(\frac{1}{2}+a\right)c_{l_\gamma}+2c_{m_\gamma}
\end{aligned}
\tag{5}
$$

Introduce the following notation: $c_1=\rho V^2 b s_p$, $c_2=\rho V^2 b^2 s_p$. Then (3), (4) take the form

$$
L = C_1\left(\alpha+\left(\frac{\dot{h}}{V}+\left(\frac{1}{2}-A\right)b\frac{\alpha}{V}\right)\right)+c_1c_{l_\beta}\beta+c_1c_{l_\gamma}\gamma \tag{6}
$$

$$
\begin{aligned}
M = c_2c_{m_{\alpha-\text{ eff}}}&\left(\alpha+\left(\frac{\dot{h}}{V}+\left(\frac{1}{2}-A\right)b\frac{\alpha}{V}\right)\right)+c_2c_{m_{\beta-\text{ eff}}}\beta\\
&+c_2c_{m_{\gamma-\text{ eff}}}\gamma
\end{aligned}
\tag{7}
$$

Introducing the state vector $x\in R^4$ as, we rewrite equations (1), (2), (6), (7).

$$
\begin{aligned}
\dot{x}_1 &= x_2\\
\dot{x}_2 &= c_{\alpha_1}x_1+c_{\alpha_{\text{nonl1}}}x_1^3+c_{\dot{\alpha}_1}x_2+c_{h_1}x_3+c_{\dot{h}_1}x_4+c_{\beta_1}\beta+c_{\gamma_1}\gamma,\\
\dot{x}_3 &= x_4\\
\dot{x}_4 &= c_{\alpha_2}x_1+c_{\alpha_{\text{nonl2}}}x_1^3+c_{\dot{\alpha}_2}x_2+c_{h_2}x_3+c_{h_2}x_4+c_{\beta_2}\beta+c_{\gamma_2}\gamma,
\end{aligned}
\tag{8}
$$

Where:

$$
\begin{aligned}
c_{\alpha_1} &= c_2m_tc_{m_{\alpha-\text{ eff}}}+c_1m_wx_\alpha bc_{l\alpha}-m_tk_1\\
c_{\alpha_{\text{nonl1}}} &= -m_tk_2\\
c_{\dot{\alpha}_1} &= c_2m_tc_{m_{\alpha-\text{ eff}}}\left(\frac{1}{2}-a\right)b\frac{1}{V}\\
&\quad+c_1m_wx_\alpha bc_{l_\alpha}\left(\frac{1}{2}-a\right)b\frac{1}{V}-c_\alpha m_t\\
c_{h_1} &= k_hm_wx_\alpha b
\end{aligned}
\tag{9}
$$

$$
\begin{aligned}
c_{\dot{h}_1} &= c_2m_tc_{m_{\alpha-\text{ eff}}}\frac{1}{V}+c_1m_wx_\alpha bc_{l_\alpha}\frac{1}{V}+c_hm_wx_\alpha b\\
c_{\beta_1} &= c_2m_tc_{m_{\beta-\text{ eff}}}+c_1m_wx_\alpha bc_{l_\beta}\\
c_{\gamma_1} &= c_2m_tc_{m_{\gamma-\text{ eff}}}+c_1m_wx_\alpha bc_{l_\gamma}
\end{aligned}
$$

http://www.doi.org/10.62341/sksp2112

$$
\begin{aligned}
c_{\alpha_2} &= -c_2 m_w x_\alpha b c_{m_{\alpha-\text{eff}}} - c_1 I_\alpha c_{l_\alpha} + m_w x_\alpha b k_1 \\
c_{\alpha_{\text{nonl2}}} &= m_w x_\alpha b k_2 \\
c_{\dot{\alpha}_2} &= -c_2 m_w x_\alpha b c_{m_{\alpha-\text{eff}}} \left(\frac{1}{2} - a\right) b \frac{1}{V} \\
&\quad - c_1 I_\alpha c_{l_\alpha} \left(\frac{1}{2} - a\right) b \frac{1}{V} + c_\alpha m_w x_\alpha b \\
c_{h_2} &= -k_h I_\alpha \\
c_{\dot{h}_2} &= -c_2 m_w x_\alpha b c_{m_{\alpha-eff}} \frac{1}{V} - c_1 I_\alpha c_{l_\alpha} \frac{1}{V} - c_h I_\alpha \\
c_{\beta_2} &= -c_2 m_w x_\alpha b c_{m_{\beta-eff}} - c_1 I_\alpha c_{l_\beta} \\
c_{\gamma_2} &= -c_2 m_w x_\alpha b c_{m_{\gamma-eff}} - c_1 I_\alpha c_{l_\gamma}
\end{aligned}
\tag{10}
$$

As an example, Table 1 shows the values of parameters.

Table 1: Numerical values of model parameters (8)

A	−0.6719	cm_γ	−0.1005
B	0.1905 m	I_α	$(m_w x^2{}_\alpha b^2 + 0.009039)$ kg m^2
c_α	0.036 kg m^2/s	$k_\alpha(\alpha)$	$12.77 + 1003\alpha^2\alpha^2$
c_h	27.43 kg/s	k_h	2844.4 N/m
cl_α	6.757	m_t	15.57 kg
cl_β	3.358	m_w	4.34 kg
cl_γ	−0.1566	s_p	0.5945 m
cm_α	0	x_α	$-(0.0998 + a)$
cm_β	−0.6719	ρ	1.225 kg/m^3

As a result of calculations according to (5), (9), (10), the parameters presented in Table 2 are obtained.

Table 2: Parameter values of equations (10) according to [19]

V	19.0625	m_w	4.3400	a	−0.6719
x_α	0.5721	cm_γ	−0.1005	b	0.1905
I_α	0.0606	c_α	0.0360	k_1	12.77
k_2	1003	c_h	27.4300	k_h	$2.844 \cdot 10^3$
cl_α	6.7570	m_t	15.57	cl_β	3.3580
cl_γ	−0.1566	s_p	0.5945	cm_α	0
cm_β	−0.6719	ρ	1.2250	cm_α-eff	−1.1615
$cm\beta$-eff	−1.9210	$cm\gamma$-eff	−0.1741	c_1	50.4130

http://www.doi.org/10.62341/sksp2112

Table 3, continued

c_2	9.6037	$c\alpha_1$	−211.39	$c\alpha$nonl1	−778.5
$c\alpha'_1$	−0.7076	ch_1	$1.3454 \cdot 10^3$	$ch'1$	12.3153
$c\beta_1$	−207.1799	$c\gamma_1$	−29.7643	$c\alpha_2$	−9.3225
$c\alpha_{nonl}2$	23.6498	$c\alpha'_2$	−0.1629	ch_2	−172.3376
$ch'2$	−2.4678	$c\beta_2$	−1.5305	$c\gamma_2$	1.2691

For a wing with uncontrolled edges, the following expressions are given in [18]:

$$L = \pi\rho b^2(\ddot{h} + V\dot{\alpha} - ba\ddot{\alpha}) + 2\pi\rho VbQC \tag{11}$$

$$M = \pi\rho b^2\left(ba\ddot{h} - Vb\left(\frac{1}{2} - a\right)\dot{\alpha} - b^2\left(\frac{1}{8} + a^2\right)\ddot{\alpha}\right) + 2\pi\rho b^2 V\left(a + \frac{1}{2}\right)QC \tag{12}$$

Where:

V: speed relative to the undisturbed flow

C: Theodorsen function, and the effective angle of attack Q is determined by the expression

$$Q = V\alpha + \dot{h} + \dot{\alpha}b\left(\frac{1}{2} - a\right) \tag{13}$$

Using the Wagner function convolution theorem, the following expression is obtained in [16]

$$L_c = \int_{-\infty}^{-\infty} C(k)f(\omega)e^{i\omega t}\mathrm{d}\omega = Q(0)\varphi(\tau) + \int_0^{\tau}\frac{\partial Q(\sigma)}{\partial\sigma}\varphi(\tau-\sigma)\mathrm{d}\sigma = \\ = Q(\tau)\varphi(0) + \int_0^{\tau} Q(\sigma)\frac{\partial\varphi(\tau-\sigma)}{\partial\sigma}\mathrm{d}\sigma. \tag{14}$$

Based on the Sears approximation [19], the Wagner function is represented in [20] as

$$\Phi(t) = c_0 - c_1e^{-c_2t} - c_3e^{-c_4t} \tag{15}$$

where $c_0 = 1$, $c_1 = 0.165$, $c_2 = 0.0455$, $c_3 = 0.335$, $c_4 = 0.3$. Using the Pade approximation [16] for the exponential function, the following formula is derived in [16]:

$$L_c = (c_0 - c_1 - c_3)Q(t) + c_2c_4(c_1 + c_3)\left(\frac{V^2}{b}\right) \\ + (c_1c_2 + c_3c_4)V\dot{x} \tag{16}$$

http://www.doi.org/10.62341/sksp2112

where are two additional variables of the model state equations, defined by the following equation (19)

$$\ddot{\bar{x}} = -c_2 c_4 \frac{V^2}{b^2}\bar{x} - (c_2 + c_4)\frac{V}{b}\dot{\bar{x}} + \frac{V}{b}\alpha + \left(\frac{1}{2} - a\right)\dot{\alpha} + \frac{\dot{h}}{b} \quad (17)$$

Using (14), (16), we obtain equations for lift force and moment as:

$$\begin{aligned} L = \pi\rho b^2(\ddot{h} + V\dot{\alpha} - ba\ddot{\alpha}) + 2\pi\rho Vb(c_0 - c_1 - c_3)Q \\ + +2\pi\rho V^3 c_2 c_4(c_1 + c_3)\bar{x} \\ + 2\pi\rho V^2 b(c_1 c_2 + c_3 c_4)\bar{x} \end{aligned} \quad (18)$$

Uncontrolled Bending Flutter Model Using Wagner's Function:
In dimensionless form, the equations for uncontrolled bending flutter are written as follows:

$$\begin{aligned} M = \pi\rho b^2\left(ba\ddot{h} - Vb\left(\frac{1}{2} - a\right)\dot{\alpha} - b^2\left(\frac{1}{8} + a^2\right)\ddot{\alpha}\right) + \\ +2\pi\rho b^2 V\left(a + \frac{1}{2}\right)(c_0 - c_1 - c_3)Q \\ + 2\pi\rho bV^3\left(a + \frac{1}{2}\right)c_2 c_4(c_1 + c_3)\bar{x} + \\ +2\pi\rho b^2 V^2\left(a + \frac{1}{2}\right)(c_1 c_2 + c_3 c_4)\bar{x} \end{aligned} \quad (19)$$

Where:
the symbol "·" denotes differentiation with respect to dimensionless time.
t_1: real time, V: air speed.
Where:
natural frequencies of isolated bending and torsional vibrations respectively.
damping coefficients.
r_α: denotes the radius of circular motion relative to the elastic axis.
stiffness coefficients for nonlinear bending and torsional stiffness respectively.
The external force and moment are denoted by.
m: mass of the wing per unit length.
In [15], it is assumed that, where (η) is the coefficient of the cubic component of torsional stiffness.
In [16], the cubic nonlinear relationship is also used for , although in the main part, a linear approximation is also used in [17] (where).

http://www.doi.org/10.62341/sksp2112

For incompressible flow, the expressions for, according to [17, 18], take the form:

$$\begin{aligned} C_L(t) &= \pi\left(\ddot{\xi} - a_h\ddot{\alpha} + \dot{\alpha}\right) \\ &\quad + 2\pi\left(\alpha(0) + \dot{\xi}(0) + \left(\frac{1}{2} - a_h\right)\dot{\alpha}(0)\right)\varphi(\tau) + \\ &\quad 2\pi\int_0^t \varphi(\tau-\sigma)\cdot\left(\dot{\alpha}(\sigma) + \ddot{\xi}(\sigma) + \left(\frac{1}{2} - a_h\right)\ddot{\alpha}(\sigma)\right)\mathrm{d}\sigma \\ C_M(t) &= \pi\left(\frac{1}{2} + a_h\right)\left(\alpha(0) + \dot{\xi}(0) + \left(\frac{1}{2} - a_h\right)\dot{\alpha}(0)\right)\varphi(\tau) \\ &+\pi\left(\frac{1}{2} + a_h\right)\int_0^t \varphi(t-\sigma) \\ &\quad \cdot\left(\dot{\alpha}(\sigma) + \ddot{\xi}(\sigma) + \left(\frac{1}{2} - a_h\right)\ddot{\alpha}(\sigma)\right)\mathrm{d}\sigma \\ &\quad +\frac{\pi}{2}a_h\left(\ddot{\xi} - a_h\ddot{\alpha}\right) - \left(\frac{1}{2} - a_h\right)\frac{\pi}{2}\dot{\alpha} - \frac{\pi}{16}\ddot{\alpha} \end{aligned} \tag{20}$$

where the Wagner function is represented by the following John approximation [16].

To eliminate the integral terms in (19), (20), new variables are introduced [16, 17]:

$$\begin{aligned} w_1 &= \int_0^t \mathrm{e}^{\varepsilon_1(t-\sigma)}\alpha(\sigma)\mathrm{d}\sigma,\ w_2 = \int_0^t \mathrm{e}^{\varepsilon_2(t-\sigma)}\alpha(\sigma)\mathrm{d}\sigma \\ w_3 &= \int_0^t \mathrm{e}^{\varepsilon_1(t-\sigma)}\xi(\sigma)\mathrm{d}\sigma,\ w_4 = \int_0^t \mathrm{e}^{\varepsilon_2(t-\sigma)}\xi(\sigma)\mathrm{d}\sigma \end{aligned} \tag{21}$$

Then the system (19) takes the form [19]

$$\begin{aligned} c_0\ddot{\xi} + c_1\ddot{\alpha} + c_2\dot{\xi} + c_3\dot{\alpha} + c_4\xi + c_5 + c_6w_1 + c_7w_2 + c_8w_3 \\ + +c_9w_4 + c_{10}G(\xi) = f(t) \\ d_0\ddot{\xi} + d_1\ddot{\alpha} + d_2\dot{\xi} + d_3\dot{\alpha} + d_4\xi + d_5\alpha + d_6w_1 + d_7w_2 \\ + d_8w_3 + d_9w_4 + d_{10}M(\alpha) = g(t \end{aligned} \tag{22}$$

Where the functions depend on initial conditions, Wagner functions and external influences.

Nonlinear restoring forces have the form, with coefficients γ, η, and the coefficients ci, di, i= 0, …,10 is described as follows expressions [10]:

$$c_0 = 1 + \frac{1}{\mu},\ c_1 = x_\alpha - \frac{a_h}{\mu},\ c_2 = \frac{2}{\mu}(1 - \psi_1 - \psi_2) + 2\zeta_\zeta\frac{\bar{\omega}}{V^*} \tag{23}$$

http://www.doi.org/10.62341/sksp2112

$$c_3 = \frac{1}{\mu}\left(1 + (1-2a_h)(1-\psi_1-\psi_2)\right),\ c_4 = \frac{2}{\mu}(\varepsilon_1\psi_1 + \varepsilon_2\psi_2)$$

$$c_5 = \frac{2}{\mu}\left(1-\psi_1-\psi_2+\left(\frac{1}{2}-a_h\right)(\varepsilon_1\psi_1+\varepsilon_2\psi_2)\right)$$

$$c_6 = \frac{2}{\mu}\varepsilon_1\psi_1\left(1-\varepsilon_1\left(\frac{1}{2}-a_h\right)\right),\ c_7 = \frac{2}{\mu}\varepsilon_2\psi_2\left(1-\varepsilon_2\left(\frac{1}{2}-a_h\right)\right)$$

$$c_8 = -\frac{2}{\mu}\varepsilon_1^2\psi_1,\ c_9 = -\frac{2}{\mu}\varepsilon_2^2\psi_2,\ c_{10} = \left(\frac{\bar{\omega}}{V^*}\right)^2$$

$$d_0 = \frac{x_\alpha^2}{r_\alpha^2} - \frac{a_h}{\mu r_\alpha^2},\ d_1 = 1 + \frac{1+8a_h^2}{8\mu r_\alpha^2},\ d_2 = -\frac{1+2a_h}{\mu r_\alpha^2}(\varepsilon_1\psi_1+\varepsilon_2\psi_2)$$

$$d_3 = \frac{1-2a_h}{2\mu r_\alpha^2} - \frac{(1-4a_h^2)(1-\psi_1-\psi_2)}{2\mu r_\alpha^2} + \frac{2\zeta_\alpha}{V^*},\ d_4 = -\frac{1+2a_h}{\mu r_\alpha^2}(\varepsilon_1\psi_1+\varepsilon_2\psi_2)$$

$$d_5 = -\frac{1+2a_h}{\mu r_\alpha^2}(1-\psi_1-\psi_2) - \frac{(1+2a_h)(1-2a_h)(\psi_1\varepsilon_1-\psi_2\varepsilon_2)}{2\mu r_\alpha^2} \quad (24)$$

$$d_6 = -\frac{(1+2a_h)\psi_1\varepsilon_1}{\mu r_\alpha^2}\left(1-\varepsilon_1\left(\frac{1}{2}-a_h\right)\right),\ d_7 = \frac{(1+2a_h)\psi_2\varepsilon_2}{\mu r_\alpha^2}\left(1-\varepsilon_2\left(\frac{1}{2}-a_h\right)\right)$$

$$d_8 = \frac{(1+2a_h)\psi_1\varepsilon_1^2}{\mu r_\alpha^2},\ d_9 = \frac{(1+2a_h)\psi_2\varepsilon_2^2}{\mu r_\alpha^2},\ d_{10} = \left(\frac{1}{V^*}\right)^2$$

Introducing the state vector $x \in R^8$ with components, and assuming initially that there are no external forces, the system (22) can be rewritten as follows [19]:

$$M\ddot{x} + \mu\dot{x} + Kx + CW(x) + F(x) = 0 \quad (25)$$

Where:

http://www.doi.org/10.62341/sksp2112

$$,x = [\xi, \alpha]^{\mathrm{T}},\ W(x) = [w_1, w_2, w_3, w_4]^{\mathrm{T}},\ M = \begin{bmatrix} c_0 & c_1 \\ d_0 & d_1 \end{bmatrix},\ \mu = \begin{bmatrix} c_2 & c_3 \\ d_2 & d_3 \end{bmatrix}$$
$$K = \begin{bmatrix} c_4 + c_{10} & c_5 \\ d_4 & d_5 + d_{10} \end{bmatrix},\ C = \begin{bmatrix} c_6 & c_7 & c_8 & c_9 \\ d_6 & d_7 & d_8 & d_9 \end{bmatrix} \quad (26)$$
$$F(x) = [d_{10}\gamma\xi^3, d_{10}\eta\alpha^3]^{\mathrm{T}} = [d_{10}\gamma x_1^3, d_{10}\eta x_3^3]^{\mathrm{T}}$$

In Cauchy form, system (26) takes the form
Where:
As indicated in (26), if we take the Wagner function in the expression for Φ, then the equations for take the form

$$\begin{cases} \dot{x}_1 = x_2 \\ \dot{x}_2 = v_2 \\ \dot{x}_3 = x_4 \\ \dot{x}_4 = v_1 \\ \dot{x}_5 = -\varepsilon_1 x_5 + x_1 \\ \dot{x}_6 = -\varepsilon_2 x_6 + x_1 \\ \dot{x}_7 = -\varepsilon_1 x_7 + x_3 \\ \dot{x}_8 = -\varepsilon_2 x_8 + x_3 \end{cases} \quad (27)$$
$$v = [v_1 \quad v_2]^T = -M^{-1}(\mu \cdot [x_2 \quad x_4]^T + K[x_1 \quad x_3]^T + CW + F(x)).$$

Where
$v = [v_1 \quad v_2]^T = -M^{-1}(\mu \cdot [x_2 \quad x_4]^T + K[x_1 \quad x_3]^T + CW + F(x))$.

As indicated in [30], if we take the Wagner function $\Phi = 1$, i.e., $\psi_1 = \psi_2 = 0$ in the expression for Φ, then the equations for $C_L(t), C_m(t)$ take the form

$$C_L(t) = \pi\left(\ddot{\xi} - a_h\ddot{\alpha} + 2\dot{\xi}\left((2 - 2a_h)\dot{\alpha}\right) + 2\alpha\right.$$
$$C_M(t) = \frac{\pi}{2}\left(a_h\ddot{\xi} - \left(\frac{1}{8} + A_h^2\right)\ddot{\alpha} + (1 + 2a_h)\dot{\xi} + \right. \quad (28)$$
$$\left. A_h(1 - 2a_h)\dot{\alpha} + (1 + 2a_h)\alpha\right)$$

Then the original aeroelastic system is described as a system of four first-order differential equations. But in such an approximation, the second bifurcation phenomenon cannot be detected [19].
Modeling of Bending-Torsion Vibrations of the Wing: As an example, we present the results of modeling wing bending-torsion vibrations.

http://www.doi.org/10.62341/sksp2112

- **Model Dynamics Parameters**

Based on the data provided in [17, 18], the modeling utilized the initial parameter values listed in Table 4.

- **Simulation Results**

The initial value α (0) = 1/57.3 rad=1.0 deg was taken for the simulation, with the remaining initial conditions assumed to be zero. The processes of changing the variables $\alpha(t)$, $\xi(t)$ and the projection of phase trajectories on the plane (α,), (ξ,) are shown in Fig (4). As can be seen from the graphs, the equilibrium state of the system is unstable, and a stable limit cycle appears.

Table 4: Resulting Parameter Values for Simulation

$c_0 = 1.01$	$c_1 = 0.255$	$c_2 = 0.01$	$c_3 = 0.02$
$c_4 = 0.00216$	$c_5 = 0.01216$	$c_6 = 0.0001433$	$c_7 = 0.001407$
$c_8 = -6.832 \cdot 10^{-6}$	$c_9 = -0.000603$	$c_{10} = 0.00119$	
$d_0 = 1.02$	$d_1 = 1.015$	$d_2 = 0$	$d_3 = 0.04$
$d_4 = 0$	$d_5 = 0$	$d_6 = 0$	$d_7 = 0$
$d_8 = 0$	$d_9 = 0$	$d_{10} = 0.01904$	

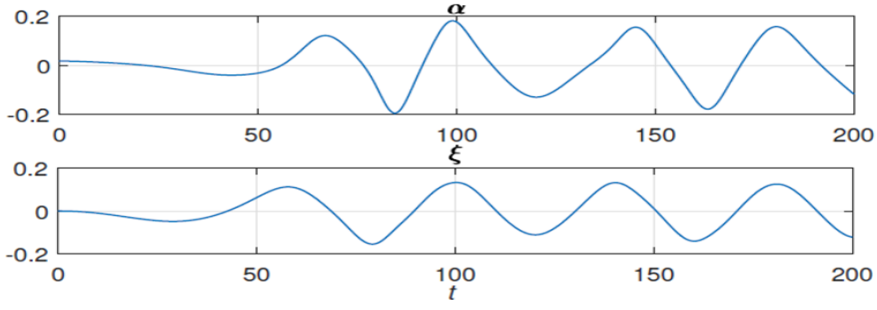

Fig 3: Processes of α(t), ξ(t) changes

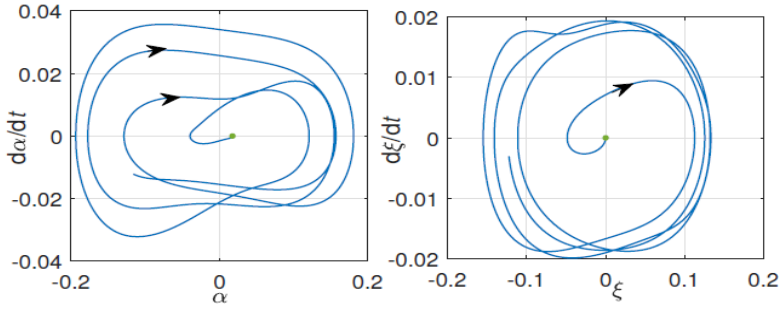

Fig 4: Projections of Phase Trajectories onto the Plane

http://www.doi.org/10.62341/sksp2112

5.2. Flutter Suppression:

Passive flutter suppression: In [15], the dependence of the critical flutter speed of a high aspect ratio wing on the position of the engines on it is studied. An approximate method of parametric studies based on the Rayleigh principle is proposed. The rational position of the engines relative to the main wing axes is determined using a simplified model in which the mass and stiffness characteristics of the wing are reduced to the selected section. A numerical example is given for calculating the critical flutter speed depending on the position of the engines on the wing.

As noted in [16], passive control strategies for flutter suppression have a significant advantage over active control strategies in terms of minimizing useful load and avoiding issues related to sensor and control surface activation. [16] focuses on passive control strategy, specifically nonlinear energy absorption (NES), aimed at suppressing or reducing the amplitude of vibrations of aeroelastic systems' limit cycle. The system under consideration consists of a rigid aerodynamic profile elastically mounted on linear and nonlinear springs.

This wing has two degrees of freedom: vertical translational motion, called plunge and denoted by h, and clockwise rotational motion, called pitch and denoted by θ. The displacement of the mass for the nonlinear energy absorber relative to the wing is denoted by y_2. The parameters $k_h(h)$, $k_\theta(\theta)$, and $k_n(y_2)$ are used to represent the stiffness of bending, twisting, and the energy absorber, respectively. They are given by the following expressions:

$$k_h(h) = k_{h_0} + k_{h_1} h + k_{h_2} + h^2 \tag{29}$$

$$k_\theta(\theta) = k_{\theta_0} + k_{\theta_1}\theta + k_{\theta_2}\theta^2 \tag{30}$$

$$k_n(y_2) = k_{n_2} {y_2}^2 \tag{31}$$

In [19], based on the energy approach and the Lagrange formalism, assuming that $y2$ is measured from the origin, the following dimensionless equations of motion for the "paired wing/energy absorber" system are obtained:

$$\begin{aligned} &\ddot{h} + e^*\ddot{\theta}\cos\theta + \frac{\sigma^2}{V^2}\left(h + \eta_1^h h^2 + \eta_2^h h^3\right) \\ &\quad + \bar{\eta}\frac{\sigma^2}{V^2}(-y_2 - d^*\sin\theta + h)^3 + \frac{\bar{C}_1}{V}\dot{h} \\ &\quad + +\overline{C_{y_2}}\frac{\sigma}{V}\left(\dot{y}_2 + d^*\dot{\theta}\cos\theta - \dot{h}\right) = -\bar{L} \end{aligned} \tag{32}$$

http://www.doi.org/10.62341/sksp2112

$$r^2\ddot{\theta} + e^*\cos(\theta)\,\ddot{h} + \bar{\varepsilon}d^{*2}\ddot{\theta} + \frac{r^2}{V^2}\left(\theta + \eta_1^{\theta}\theta^2 + \eta_2^{\theta}\theta^3\right)$$
$$-\bar{\eta}\frac{\sigma^2}{V^2}d^*\cos\theta(-y_2 - d\sin\theta + h)^3 + \frac{\overline{C_2}}{V}\dot{\theta} \qquad (33)$$
$$+\overline{C_{y_2}}\frac{\sigma}{V}d^*\cos\theta\left(\dot{y}_2 + d^*\dot{\theta}\cos\theta - \dot{h}\right) = \bar{M}$$

$$\bar{\varepsilon}\ddot{y}_2 + \bar{\eta}\frac{\sigma^2}{V^2}(y_2 + d^*\sin\theta - h)^3 \qquad (34)$$
$$+\overline{C_{y_2}}\frac{\sigma}{V}\left(\dot{y}_2 + d^*\dot{\theta}\cos\theta - \dot{h}\right) = 0$$

Where:
ε: ratio of the energy absorber mass to the total system mass.
σ: frequency ratio.
V: reduced velocity.
d: dimensionless position of the energy absorber relative to the elastic axis.

Nonlinear quasi-steady aerodynamics are used to represent aerodynamic loads. To find the lift force and moment, expressions similar to (11) - (13) are used in [19].
The parameters including mass and placement of the passive absorber, are varied to test its effectiveness in suppressing unwanted aerodynamic behavior under different conditions. A semi-quantitative assessment of aerodynamic, structural, and runoff nonlinearities depending on the type of instability is obtained. According to the results [16], depending on the mass and position along the profile, the nonlinear absorber may be more effective in terms of changing the subcritical bifurcation to supercritical. However, the change is very limited as the system reverts to subcritical response with increasing free stream velocity. For the case where the original system exhibits supercritical behavior, the results show that the nonlinear absorber can reduce the amplitudes of the primary tone and bending. However, this reduction is limited to a very small range of flow speeds above the flutter speed. Results for the normal form show that the nonlinear absorber has damping characteristics and, as such, cannot sustain the energy it absorbs from the aerodynamic airfoil section. This leads to modulated characteristics of both the aerodynamic section and the nonlinear absorber. Adding a relatively small mass to the main system, attached via a linear spring and damper (linear tuned vibration

http://www.doi.org/10.62341/sksp2112

absorber, LTVA), significantly improves the stability of the mechanical system. The use of a purely nonlinear spring in the absorber increases the absorber's frequency bandwidth, reduces the vibrations of the limit cycle, and allows avoiding subcritical bifurcations with stability loss. In [16], a nonlinear tuned vibration absorber (NLTVA) is proposed, whose restoring force is adjusted according to the functional form of the nonlinearity of the primary system. NLTVA is designed to leverage the positive features of both LTVA and nonlinear absorbers. It is shown in [16] that NLTVA can compensate for the detrimental effects of nonlinearities in the primary system, meaning the coupled system exhibits linear dynamics similar to the same system without structural nonlinearities. Considering the Van der Pol - Duffing oscillator as the primary system, an analytical solution in closed form for local compensation of nonlinearities is obtained. Numerical continuation methods have shown that compensation is also valid for large response amplitudes. The configuration with an external store of the F-16 fighter jet is examined in [19] using a time-domain aeroelasticity calculation program. The program used an Euler flow solver with medium accuracy in combination with a linear modal representation of the structure. A key feature of the program code was that it allowed the user to specify nonlinear damping profiles. Four damping profiles were investigated to determine their influence on the effectiveness of the approach considered for predicting aeroelastic vibrations of the limit cycle. Damping was specified as a function of oscillatory response, and the solution results were compared with flight test responses depending on the Mach number. Realistic limit cycle vibrations were obtained for three investigated damping profiles.

6. **Results**

The results of the calculations according to formulas (34), (35) are presented in Table 4. The processes of changing the variables $\alpha(t)$, $\xi(t)$ and the projection of phase trajectories on the plane (α,), (ξ,) are shown in Fig (4). As can be seen from the graphs, the equilibrium state of the system is unstable, and a stable limit cycle appears This is confirmed by the values of the resulting parameters of the simulation. We recommend studying Reduced Order Models and Active flutter suppression by linear-quadratic optimal controllers and Active flutter suppression using variable structure controllers and adaptive controllers.

http://www.doi.org/10.62341/sksp2112

7. Conclusion:

The provides an overview of existing results on elastic bending wing flutter. Models of elastic bending wing flutter are presented, including equations for the deflection and twist of a flat wing, The model for the aerodynamic combination of the airfoil and aileron, an approximate description of the lift-weight function of converging wings in an incompressible flow, a model of uncontrolled bending flutter through the Wagner function, as well as reduced-order models. The exposition is illustrated with the results of modeling of bending-torsional wing vibrations. Research on the phenomenon of elastic bending wing flutter is described, including numerical and experimental studies. Several approaches to passive flutter suppression are considered.

References:

[1] M.R.Amoozgar,S.A.Fazelzadeh, H.HaddadKhodaparast, M.I.Friswell, J.E.Cooper, Aeroelastic stability analysis of aircraft wings with initial curvature, Elsevier, Aerospace Science and Technology (2020) 1270-9638.

[2] P. Mardanpour, D.H. Hodges, R. Neuhart, N. Graybeal, Engine placement effect on nonlinear trim and stability of flying wing aircraft, J. Aircr. 50(6) (2013) 1716–1725.

[3] P. Mardanpour, E. Izadpanahi, S. Rastkar, S.A. Fazelzadeh, D.H. Hodges, Geo-metrically exact, fully intrinsic analysis of pre-twisted beams under distributed follower forces, AIAA J. 56(2) (2017) 836–848.

[4] M.R. Amoozgar, H. Shahverdi, Analysis of nonlinear fully intrinsic equations of geometrically exact beams using generalized differential quadrature method, Acta Mech. 227(5) (2016) 1265–1277.

[5] M.R. Amoozgar, H. Shahverdi, A.S. Nobari, Aeroelastic stability of hingeless rotor blades in hover using fully intrinsic equations, AIAA J. 55(7) (2017) 2450–2460.

[6] M.A. De Rosa, C. Franciosi, Exact and approximate dynamic analysis of circular arches using DQM, Int. J. Solids Struct. 37(8) (2000) 1103–1117.

http://www.doi.org/10.62341/sksp2112

[7] Starossek U, Starossek RT. Parametric flutter analysis of bridges stabilized with eccentric wings. J Wind Eng Industr Aerodynam. 2021; 211:104566.

[8] L. Bairstow, A. Fage, Oscillation of the tailplaneand body of an aeroplane in flight, A.R.C. R. & M. 276(part 2) (1916).

[9] M. Goland, The flutter of a uniform cantilever wing, J. Appl. Mech. 12(4) (1945) A197–A208.

[10] M. Goland, Y.L. Luke, The flutter of a uniform wing with tip weights, J. Appl. Mech. 15 (1948) 13–20.

[11] D. Li, S. Zhao, A. Da Ronch, J. Xiang, J. Drofelnik, Y. Li, L. Zhang, Y. Wu, M. Kintscher, H.P. Monner, A. Rudenko, S. Guo, W. Yin, J. Kirn, S. Storm, R.D. Breuker, A review of modelling and analysis of morphing wings, Prog. Aerosp. Sci. 100 (2018) 46–62.

[12] S. Barbarino, O. Bilgen, R.M. Ajaj, M.I. Friswell, D.J. Inman, A review of morph-ing aircraft, J. Intell. Mater. Syst. Struct. 22(9) (2011) 823–877.

[13] I. Lottati, Aeroelastic stability characteristics of a composite swept wing with tip weights for an unrestrained vehicle, J. Aircr. 24(11) (1987) 793–802.

[14] C. Panda, Venkatasubramani SRP, Aeroelasticity- In General and Flutter Phenomenon, Second International Conference on Emerging Trends in Engineering and Technology, ICETET-09 (2009) 978-0-7695-3884-6/09.

[15] Дулина Н.Г. Исследование влияния параметров компоновки крыла с двигателями на величину критической скорости флаттера // Ученые записки ЦАГИ. 1979. Т. X, № 6. С. 90–98.

[16] Bichiou Y., Hajj M., Nayfeh A. Effectiveness of a nonlinear energy sink in the control of an aeroelastic system // Nonlinear Dynamics. 2016. Vol. 86, no. 4. P. 2161–2177.

[17] Liu L. P., Dowell E. H. The secondary bifurcation of an aeroelastic airfoil motion: effect of high harmonics // Nonlinear Dynamics. 2004. Vol. 37, no. 1. P. 31–49.

[18] Zhang Y., Chen Y., Liu J., Meng G. Highly Accurate Solution of Limit Cycle Oscillation of an Airfoil in Subsonic Flow // Advances in Acoustics and Vibration. 2011. Vol. 2011, no. ID 926271. P. 1–10.

http://www.doi.org/10.62341/sksp2112

[19] Chen C.-L., Peng C. C., Yau H.-T. High-order sliding mode controller with backstepping design for aeroelastic systems // Communications in Nonlinear Science and Numerical Simulation. 2012. Vol. 17, no. 4. P. 1813 – 1823. URL: http://www.sciencedirect.com/ science/article/pii/S1007570411005028.